Exhibit B

THE JOURNAL OF BIOLOGICAL CHEMISTRY
Vol. 277, No. 32, Issue of August 9, pp. 28909–28915, 2002
Printed in U.S.A.

Evidence That the Human Gene for Prostate Short-chain Dehydrogenase/Reductase (*PSDR1*) Encodes a Novel Retinal Reductase (RalR1)*

Received for publication, March 18, 2002, and in revised form, May 24, 2002
Published, JBC Papers in Press, May 29, 2002, DOI 10.1074/jbc.M202588200

Natalia Y. Kedishvili‡§, Olga V. Chumakova‡, Sergei V. Chetyrkin‡¶, Olga V. Belyaeva‡, Elena A. Lapshina‡, Daniel W. Lin‖, Masazumi Matsumura**, and Peter S. Nelson**‡‡**

*From the ‡Division of Molecular Biology and Biochemistry, School of Biological Sciences, University of Missouri-Kansas City, Kansas City, Missouri 64110, the Departments ‖Urology and ‡‡Medicine, University of Washington, Seattle, Washington 98195, and the **Division of Human Biology, Fred Hutchinson Cancer Research Center, Seattle, Washington 98109*

All-*trans*-retinoic acid is a metabolite of vitamin A (all-*trans*-retinol) that functions as an activating ligand for a family of nuclear retinoic acid receptors. The intracellular levels of retinoic acid in tissues are tightly regulated, although the mechanisms underlying the control of retinoid metabolism at the level of specific enzymes are not completely understood. In this report we present the first characterization of the retinoid substrate specificity of a novel short-chain dehydrogenase/reductase (SDR) encoded by *RalR1/PSDR1*, a cDNA recently isolated from the human prostate (Lin, B., White, J. T., Ferguson, C., Wang, S., Vessella, R., Bumgarner, R., True, L. D., Hood, L., and Nelson, P. S. (2001) *Cancer Res.* 61, 1611–1618). We demonstrate that RalR1 exhibits an oxidoreductive catalytic activity toward retinoids, but not steroids, with at least an 800-fold lower apparent K_m values for $NADP^+$ and NADPH *versus* NAD^+ and NADH as cofactors. The enzyme is ~50-fold more efficient for the reduction of all-*trans*-retinal than for the oxidation of all-*trans*-retinol. Importantly, RalR1 reduces all-*trans*-retinal in the presence of a 10-fold molar excess of cellular retinol-binding protein type I, which is believed to sequester all-*trans*-retinal from nonspecific enzymes. As shown by immunostaining of human prostate and LNCaP cells with monoclonal anti-RalR1 antibodies, the enzyme is highly expressed in the epithelial cell layer of human prostate and localizes to the endoplasmic reticulum. The enzymatic properties and expression pattern of RalR1 in prostate epithelium suggest that it might play a role in the regulation of retinoid homeostasis in human prostate.

All-*trans*-retinoic acid is a metabolite of vitamin A (all-*trans*-retinol) that functions as an activating ligand for a family of nuclear retinoic acid receptors (1). In target tissues, all-*trans*-retinoic acid is produced by the oxidation of all-*trans*-retinaldehyde catalyzed by cytosolic aldehyde dehydrogenases (Fig. 1) (2–5). Retinaldehyde, in turn, can be produced either by the oxidation of retinol catalyzed by microsomal or cytosolic retinol dehydrogenases (reviewed in Refs. 6 and 7) or by a symmetrical cleavage of β-carotene (Fig. 1) (8). In the small intestine, the majority of absorbed β-carotene is converted directly to all-*trans*-retinal by cytosolic β,β-carotene 15,15′-dioxygenase (9). All-*trans*-retinal produced from β-carotene is reduced to all-*trans*-retinol by microsomal retinal reductase activity (10). The enzyme that catalyzes this reaction in the small intestine functions in the presence of cellular retinol binding protein type II (CRBPII),[1] which is expressed specifically in the small intestine and binds all-*trans*-retinal with high affinity (K_d of ~100 nM) (11). Retinol produced from retinal by retinal reductase is then esterified by lecithin-retinol acyltransferase and incorporated into the lipid core of the chylomicron (12). The retinyl esters associated with chylomicrons are cleared into hepatocytes where they undergo a cycle of hydrolysis and re-esterification before storage (12).

It is generally believed that retinol secreted from the liver bound to plasma retinol-binding protein serves as the major source of retinoids for peripheral tissues (8). However, there is growing evidence that a number of cell types are capable of utilizing β-carotene directly, supplementing their own retinoid stores even though serum levels of retinol are tightly controlled. For instance, in addition to the small intestine, β-carotene is converted to retinol in the liver (8), human colon cancer cells (13), and human lung (14) and skin fibroblasts (15).

Significant progress in understanding the tissue-specific uptake and metabolism of β-carotene was provided through the molecular characterization of β,β-carotene 15,15′-dioxygenases from the fruit fly (16), chicken (17), mouse (18, 19), and human (20). Northern blot analysis of the corresponding mRNAs revealed that, besides the small intestine, many tissues, including liver, kidney, brain, stomach, testis, and small intestine express relatively high levels of β,β-carotene 15,15′-dioxygenase (17–20). *In situ* hybridization analysis of β-carotene dioxygenase expression showed that the corresponding mRNA was expressed primarily in epithelial structures of tissues such as duodenum, lung, and kidney as well as in skin, where it could serve to provide the tissue-specific vitamin A supply (21). Re-

* This work was supported by the National Institute on Alcohol Abuse and Alcoholism Grants AA00221 and AA12153 (to N. Y. K.) and by NCI, National Institutes of Health Grant CA75173 and Department of Defense Grant PC991274 (to P. S. N.). The costs of publication of this article were defrayed in part by the payment of page charges. This article must therefore be hereby marked "*advertisement*" in accordance with 18 U.S.C. Section 1734 solely to indicate this fact.

§ To whom correspondence should be addressed: Division of Molecular Biology and Biochemistry, School of Biological Sciences, University of Missouri-Kansas City, 5007 Rockhill Rd., 103 BSB, Kansas City, MO 64110. Tel.: 816-235-2658; Fax: 816-235-5595; E-mail: kedishvilin@umkc.edu.

¶ Present address: Dept. of Biochemistry and Molecular Biology, The University of Kansas Medical Center, 3901 Rainbow Blvd., Kansas City, KS 66160-7421.

[1] The abbreviations used are: CRBPII, cellular retinol binding protein type II; SDR, short-chain dehydrogenase/reductase; mAb, monoclonal antibody; BSA, bovine serum albumin; CMV, cytomegalovirus; PBS, phosphate-buffered saline; Endo H, endoglycosidase H; HPLC, high performance liquid chromatography; ER, endoplasmic reticulum.

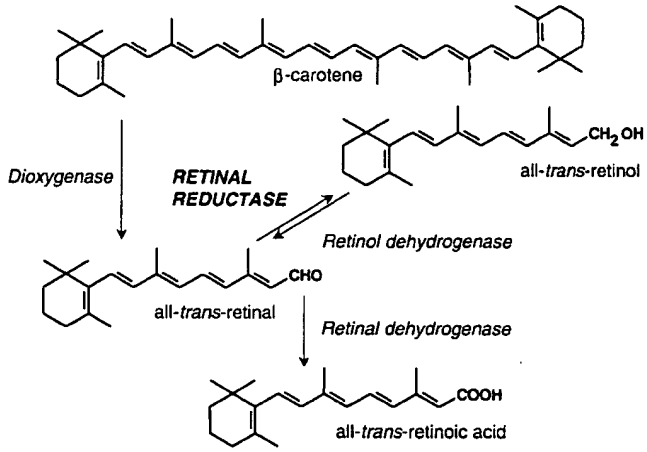

FIG. 1. **Biosynthesis of retinoic acid from β-carotene.**

cently, prostate epithelial cell lines LNCaP, PC-3, and DU 145 were shown to convert β-carotene to retinol (22), suggesting that human prostate epithelium also contains β-carotene dioxygenase. However, the one or more enzymes responsible for the reduction of retinal produced from β-carotene to retinol in prostate as well as other tissues have yet to be characterized. Furthermore, the enzyme responsible for the intestinal microsomal retinal reductase activity that recognizes CRBPII-bound retinal as substrate has not yet been defined at the molecular level.

Recently, we have shown that the prostate expresses high levels of a transcript encoding a novel member of the short-chain dehydrogenase/reductase (SDR) superfamily, *PSDR1* (23). In the present study we characterized the cell-specific expression, subcellular localization, and catalytic properties of the protein encoded by the human *PSDR1* gene. We present evidence that PSDR1 is a microsomal retinal reductase that is expressed in the epithelial cells of the human prostate gland and is capable of reducing all-*trans*-retinal to all-*trans*-retinol under physiologically relevant conditions. This activity suggests that PSDR1 might contribute to the enzymatic conversion of retinaldehyde produced from β-carotene to retinol in human prostate. To provide a nomenclature more descriptive of actual biochemical activity, we have changed the designation of this gene and encoded protein from *PSDR1* to *RalR1* for Retinal Reductase 1.

EXPERIMENTAL PROCEDURES

RalR1 Monoclonal Antibody—A peptide located near the C terminus of RalR1, CH_3CO-CHVAWVEQARNETIAR-$CONH_2$ (residues 287–303), was synthesized (Genemed Synthesis, Inc., South San Francisco, CA) and conjugated to maleimide-activated keyhole limpet hemocyanin (Pierce, Rockford, IL) through the N-terminal Cys of the peptide. Mice were immunized with the keyhole limpet hemocyanin-peptide conjugate, and a monoclonal antibody (mAb) was generated in the Biologics Production Facility of the Fred Hutchinson Cancer Research Center. Hybridomas were screened by enzyme-linked immunosorbent assay using bovine serum albumin (BSA) conjugated with the RalR1 peptide as a positive control and BSA conjugated with unrelated peptides as negative controls. Positive clones were further screened by immunoblotting using COS-7 cells transfected with RalR1 expression vectors. One hybridoma clone producing RalR1-specific mAb, designated H8, was used throughout this study.

Immunostaining of Human Prostate—Six-micron sections of formalin-fixed, paraffin-embedded blocks of prostate tissue were deparaffinized and rehydrated in sequential solutions of xylene and ethanol. The sections were sequentially immersed in a 3% aqueous solution of hydrogen peroxide to inactivate endogenous peroxidase activity, a 1% solution of bovine serum albumin in phosphate-buffered saline to block nonspecific protein binding, and then microwaved for 15 min in a 10 mM citrate buffer to "unmask" antigenicity. The sections were immunostained using a three-step indirect avidin-biotin-peroxidase method. The primary antibody was mouse monoclonal anti-RalR1, which was affinity-purified on a protein G column. The negative controls for antibody specificity consisted of non-immune mouse serum and coincubation of the anti-RalR1 antibody with 10-fold molar excess of RalR1 peptide for 2 h before subsequently incubating the monoclonal antibody/peptide solution with tissue sections. Immunoreactivity of the primary antibody was detected using an avidin-biotin-peroxidase kit (Dako Corp., Carpinteria, CA). The diaminobenzidine reaction product was enhanced with an 8% aqueous solution of nickel chloride, which yields a black reaction product. The sections were counterstained with a methyl green nuclear stain prior to coverslipping.

RalR1 Subcellular Localization—A chimeric RalR1-FLAG-tagged protein was constructed by amplifying the full-length RalR1 coding sequence by the PCR using primers PSDR1–5 (5′-TTAAGCTTGCGGC-CGCGAATTCCCACC-3′) and PSDR1–3 (5′-TCACTATCTAGAGTC-TATTGGGAGGCCCAGCAG-3′). The product was sequence-verified, cleaved with *Not*I and *Xba*I enzymes, and cloned into the p3XFLAG-CMV-14 expression vector (Sigma-Aldrich, St. Louis, MO). COS-7 monkey kidney cells (American Type Culture Collection, Manassas, VA) were grown on eight-well culture slides and transiently transfected with RalR1-FLAG using FuGENE 6 transfection reagent according to a protocol supplied by the manufacturer (Roche Molecular Biochemicals, Indianapolis, IN). Twenty-four hours after transfection, cells were washed with PBS and then fixed with 30% acetone/70% methanol mixture for 10 min at −20 °C. The cells were soaked in 3% BSA/PBS for 1 h for blocking. The primary antibody, either anti-RalR1 or M2 anti-FLAG (Sigma), was added at 1–3 μg/ml and incubated for 1 h at room temperature. The cells were washed five times with PBS containing 0.1% Tween-20 and incubated with anti-mouse IgG-conjugated with biotin (Pierce) for 30 min, followed by incubation with streptavidin-fluorescein isothiocyanate conjugate (Pierce). The cells were washed five times with PBS plus 0.1% Tween-20 between the incubations. The same immunostaining procedure was followed using the anti-RalR1 antibody on LNCaP cells grown using growth conditions suggested by the supplier (American Type Culture Collection). Mounting medium (Vector Laboratories, Inc., Burlingame, CA) was applied to each well, and the slides were immediately examined using a fluorescence microscope (Olympus) equipped with a wide-field deconvolution system (DeltaVision, Applied Precision Incorporated, Issaquah, WA). Typically, 30 images were collected per section with a plane width of 0.2 μm per image through the cell center.

Expression in Sf9 Cells—The coding region of the cDNA for human RalR1 was cloned into *Eco*RI restriction site of pVL1393 Baculovirus transfer vector. The *RalR1*-pVL1393 construct with the correct orientation of the insert was selected based on restriction endonuclease digest analysis and was confirmed by DNA sequencing. Cotransfection of Sf9 cells with the transfer vector and linearized BaculoGold DNA was performed according to the manufacturer's protocol (BD PharMingen, San Diego, CA). The recombinant virus was amplified and used to produce RalR1 protein essentially as described previously for human RoDH-4 (24). The subcellular fractions were isolated by sequential centrifugations of the cell homogenate prepared using French press. The unbroken cells, cellular debris, and nuclei were removed by centrifugation at 1,000 × *g* for 10 min. Mitochondria were pelleted by centrifugation at 10,000 × *g* for 30 min, and microsomal fraction was isolated by centrifugation at 105,000 × *g* for 1 h through a 0.6 M sucrose cushion. Microsomes were resuspended in 0.1 M potassium phosphate, pH 7.4, 0.1 mM EDTA, 1 mM dithiothreitol, 20% glycerol, aliquoted, and stored frozen at −70 °C. Protein concentration was determined by Lowry *et al.* (25) using bovine serum albumin as a standard.

Western Blot Analysis, Endoglycosidase H Treatment, and Coupled in Vitro Transcription/Translation—Western blot analysis of RalR1 expression was performed using a 1:100 dilution of RalR1 mAb. Protein was detected using ECL Western blotting analysis system (Amersham Biosciences, Piscataway, NJ) as described previously (26). For endoglycosidase H (Endo H) treatment, 20 μg of microsomal protein was resuspended in 50 mM sodium phosphate buffer, pH 5.5, containing 0.1% SDS, and 0.1 M 2-mercaptoethanol. The protease inhibitor phenylmethylsulfonyl fluoride was added to a 5 mM final concentration. One half of the mixture was treated with 2.5 μl (12.5 units) of Endo H (Roche Molecular Biochemicals), and the other half received 2.5 μl of the buffer. Both samples were incubated overnight at room temperature, then denatured with SDS-PAGE loading buffer for 5 min at 94 °C and analyzed by Western blotting. 11β-Hydroxysteroid dehydrogenase type 1 with the FLAG epitope MDYKDDDD-COOH (Sigma) attached to the C terminus served as a positive control for glycosylation in Sf9 cells and deglycosylation by Endo H.

For *in vitro* protein synthesis, RalR1 cDNA cloned into pCR2.1-

TOPO vector (Invitrogen) was subjected to transcription by T7 RNA polymerase and translation in reticulocyte lysate in the presence or absence of dog pancreas microsomes (TNT Quick system, Promega, Madison, WI) according to the manufacturer's instructions. In a typical assay, 0.5–1 μg of plasmid DNA, 20 μCi of [^{35}S]methionine (Amersham Biosciences) and 0.5–1 μl of canine pancreatic microsomal membranes (Promega) were incubated for 60–90 min at 30 °C in a final volume of 12.5 μl. ^{35}S-Labeled proteins were subjected to 12% SDS-PAGE and analyzed by autoradiography.

Analysis of Enzymatic Activity—Catalytic activity of RalR1 was assayed in 90 mM potassium phosphate, pH 7.4, and 40 mM KCl at 37 °C (reaction buffer) in siliconized glass tubes as described previously (24). The oxidative and reductive activity of RalR1 toward retinoid substrates was analyzed using all-*trans* and *cis* isomers of retinoids (Sigma-Aldrich). The stock solutions of retinoid substrates were prepared in ethanol, and their concentrations were determined based on the corresponding extinction coefficients at the appropriate wavelengths. Ethanol-dissolved retinoids were solubilized in the reaction buffer by a 10-min sonication in the presence of equimolar delipidated bovine serum albumin. The concentration of ethanol in the reaction mixture did not exceed 0.3%. At this concentration, ethanol had no effect on RalR1 activity. The 500-μl reactions were started by the addition of cofactor and carried out for 15–30 min at 37 °C. The amount of protein in the reaction mixture varied from 1 to 250 μg. The reactions were terminated by the addition of an equal volume of cold ethanol supplemented with 100 μg/ml butylated hydroxytoluene. Retinoids were extracted using solid-phase extraction on a Waters Sep-Pak C18 (light) column as described before (27) and analyzed using a Waters Alliance HPLC system. Elution was monitored at 350 nm with a Waters 2487 Dual Absorbance Detector. Unless stated otherwise, retinoids were separated using normal-phase HPLC. The stationary phase was Waters Spherisorb S3W column (4.6 mm × 100 mm), and the mobile phase consisted of hexane:acetone (90:10, v/v). The flow rate was 1 ml/min. Under these conditions, all-*trans*-retinaldehyde and all-*trans*-retinol eluted at 2.09 and 4.095 min, respectively. The peak detection limits were ~1.0 pmol for all-*trans*-retinal and ~2.5 pmol for all-*trans*-retinol. The elution times for other isomers were as follows: 3.96 min for 9-*cis*-retinol, 3.28 min for 13-*cis*-retinol, 1.94 min for 9-*cis*-retinaldehyde, and 1.83 min for 13-*cis*-retinaldehyde. Retinoids were quantitated by comparing their peak areas to a calibration curve constructed from the peak areas of a series of standards.

The oxidative and reductive activity of RalR1 toward steroids was analyzed using tritiated steroids (PerkinElmer Life Sciences, Boston, MA, ~40–60 Ci/mmol each), which were diluted with cold steroids (Steraloids Inc., Newport, RI, and Sigma-Aldrich) dissolved in Me_2SO (<1% in the reaction mix) (24, 26, 27). Dihydrotestosterone (5α-androstan-17β-ol-3-one), progesterone (4-pregnen-3,20-dione), corticosterone (4-pregnen-11β,21-diol-3,20-dione), aldosterone (4-pregnen-11β,21-diol-3,18,20-trione), androsterone (5α-androstan-3α-ol-17-one), dehydroepiandrosterone (5-androsten-3β-ol-17-one), allopregnanolone (5α-pregnan-3α-ol-20-one), and 3α-androstanediol (5α-androstan-3α,17β-diol) were tested as substrates either in the oxidative direction in the presence of 1 mM NADP$^+$/NAD$^+$ or in the reductive direction in the presence of 1 mM NADPH/NADH. The amount of microsomal protein in the reaction mixture varied from 25 to 250 μg. Control reactions contained the same amount of microsomal protein isolated from Sf9 cells that were infected with wild-type virus. The 250-μl reactions were started with the addition of cofactor and incubated at 37 °C for 15–120 min. The reaction products were extracted and separated by development in chloroform:ethyl acetate (3:1, v/v) on silica gel TLC plates. After drying, TLC plates were exposed to a PhosphorImager tritium screen and analyzed using a PhosphorImager (Amersham Biosciences).

Determination of Kinetic Constants—Steady-state kinetic analysis was performed in 90 mM potassium phosphate, pH 7.4, and 40 mM KCl at 37 °C as described above. The reaction rate was linearly proportional to the amount of microsomes added per 500-μl reaction volume with up to 2 μg of protein in the reductive direction and with up to at least 10 μg of protein in the oxidative direction during the 15-min incubation time. Kinetic analysis of substrates in the reductive direction was performed with 0.625 μg of protein and in the oxidative direction with 7.5 μg per 500-μl reaction volume, so that the amount of product formed after 15 min of incubation did not exceed 10% of the initial substrate amount. Under these conditions, the background level of product formed by microsomes from Sf9 cells infected with wild-type virus did not exceed the "minus cofactor" value obtained with the same amount of enzyme-containing microsomes. A control without added cofactor was included for each concentration of substrate and was subtracted from each experimental data point. The amount of product formed in the presence of cofactor was at least 3-fold higher than that in the "minus cofactor" control. The apparent K_m values for oxidation and reduction of retinoids were determined at a fixed NADP$^+$ (1 mM) or NADPH (0.5 mM) concentrations. Each K_m determination was repeated at least three times using six concentrations of each substrate: all-*trans*-retinal (0.25–2.5 μM); 13-*cis*-retinal (0.2–2.5 μM); 9-*cis*-retinal (0.062–2.5 μM); and all-*trans*-retinol (0.5–10 μM). The values of initial velocities (nmol/min of product formed per mg of protein) were obtained by non-linear regression analysis. The apparent K_m values for cofactors were determined at a fixed saturating concentration of all-*trans*-retinal or all-*trans*-retinol with five concentrations of each cofactor: NADPH (0.125–25 μM), NADH (0.0625–2.0 mM), NADP$^+$ (1.25–15 μM), and NAD$^+$ (0.25–3 mM).

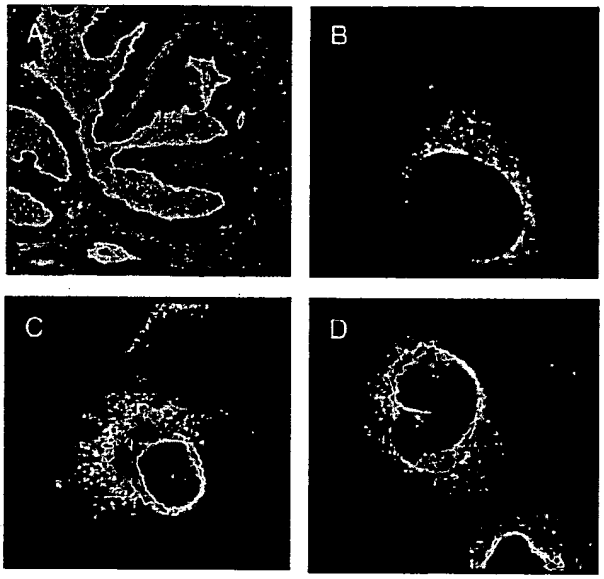

FIG. 2. **Cellular and subcellular distribution of RalR1 protein.** *A*, representative section demonstrating the expression of endogenous RalR1 protein in normal prostate tissue. High immunoreactivity is apparent in the luminal and basal epithelial cells (*black* reaction product). Stromal fibroblast and smooth muscle cell immunoreactivity was not observed. *B*, expression of endogenous RalR1 protein in the LNCaP prostate cancer cell line. Microscopic image of COS-7 cells transfected with RalR1-FLAG fusion construct and processed for FLAG (*C*) or RalR1 (*D*) immunoreactivity. The pattern of RalR1 expression localizes to the endoplasmic reticulum.

CRBPI was expressed in *Escherichia coli* as a fusion protein with glutathione *S*-transferase and purified using glutathione agarose column as described previously (28). The purified fusion protein was cleaved with thrombin and separated from glutathione *S*-transferase on a Q-Sepharose column by elution with a 0 to 500 mM NaCl gradient in 10 mM Tris, pH 7.4. The amount of functional protein was determined from the fluorescence titration curve of apo-CRBPI with retinol (29). Typically, over 90% of purified CRBPI preparation was capable of binding all-*trans*-retinol (24, 28).

RESULTS

Expression of RalR1 in Prostate Epithelium—We have previously shown that transcripts encoding RalR1 were most highly expressed in the normal prostate gland relative to all other human tissues (23). To localize the one or more specific prostate cell types expressing RalR1, we immunostained normal prostate tissue with anti-RalR1 monoclonal antibodies. High levels of RalR1 protein expression were detected in luminal epithelial cells (Fig. 2*A*). Staining was also present in basal epithelium with undetectable staining in the smooth muscle and fibroblast components of the prostate stroma. This result indicated that the novel SDR protein, RalR1, was specifically expressed in the epithelial cells of human prostate.

Subcellular Localization of RalR1 in Eukaryotic Cells—The retinal reductase activity described previously in the rat small intestine was associated with the microsomal membranes (10).

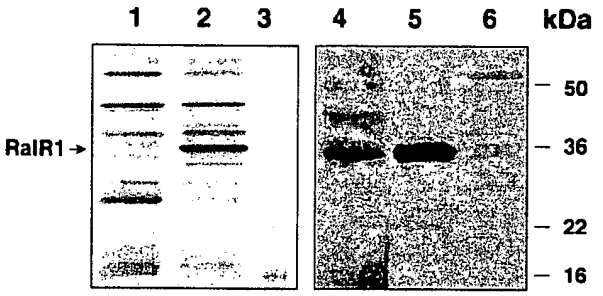

FIG. 3. **Characterization of RalR1 protein.** *Lanes 1–3*, SDS-PAGE analysis of the expressed protein in Sf9 microsomes: *lane 1*, wild-type Sf9 microsomes (10 μg); *lane 2*, Sf9 microsomes containing RalR1 (10 μg); *lane 3*, SeeBlue Plus2 pre-stained protein molecular weight standards (Invitrogen). *Lane 4*, ^{35}S-labeled RalR1 synthesized *in vitro* using coupled transcription/translation system (1.25 μl of reaction). *Lanes 5* and *6*, Western blot analysis of RalR1-containing Sf9 microsomes (*lane 5*, 10 μg) and wild-type virus infected Sf9 microsomes (*lane 6*, 10 μg). Antibodies were used at a 1:100 dilution.

To determine the subcellular localization of RalR1, we immunostained the human prostate carcinoma cell line LNCaP with anti-RalR1 antibody (Fig. 2*B*). The immunofluorescent signals (*green*) were localized to the endoplasmic reticulum (ER), indicating that RalR1 was expressed and retained in the ER. RalR1 expression in LNCaP cells was higher than in PC3 prostate carcinoma cells (data not shown), a cell type that we have previously shown expresses low levels of RalR1 message (23). To obtain further evidence for the association of RalR1 with the ER membranes, we determined whether a recombinant RalR1 was also targeted to the ER in non-prostate cell line. COS-7 cells were transfected with a construct expressing the recombinant RalR1 polypeptide fused to a 3×-FLAG tag and immunostained with the M2 anti-FLAG antibody. RalR1 expression again localized to the ER of COS-7 cells (Fig. 2*C*). To confirm this finding, COS cells transfected with RalR1 were immunostained with anti-RalR1 mAb (Fig. 2*D*). The pattern of immunofluorescence was indistinguishable from the pattern observed with the anti-FLAG antibody. These results indicated that RalR1 polypeptide contained the ER targeting signal and appeared to be associated with the ER membranes, similar to the rat intestinal retinal reductase.

Expression of the Human RalR1 Protein in Sf9 Cells—The next objective was to determine whether RalR1 was active toward retinoid substrates. We expressed the full-length cDNA for RalR1 in insect Sf9 cells using the BaculoGold Baculovirus system. Sf9 cells were homogenized and fractionated into mitochondria, microsomes, and cytosol. The subcellular localization of the recombinant protein in Sf9 cells was determined by Western blot analysis using monoclonal antibodies against RalR1. The majority of the immunoreactive protein was associated with the microsomal fraction (Fig. 3, *lanes 2* and *5*), indicating that RalR1 was targeted to the ER. At the same time, control microsomes isolated from Sf9 cells infected with wild-type virus were not stained with anti-RalR1 mAbs (Fig. 3, *lane 6*).

Because RalR1 localized to the microsomes, we investigated whether it was exposed to the lumenal side of the membrane by examining its glycosylation state. The RalR1 polypeptide contains two *N*-linked glycosylation motifs at Asn^{174} (^{174}NVS^{176}) and Asn^{298} (^{298}NET^{300}). Glycosylated proteins can be detected by their slower electrophoretic mobility relative to that of the non-glycosylated forms. Treatment of microsomal RalR1 expressed in Sf9 cells with Endo H did not change the mobility of the protein (data not shown), indicating that RalR1 was not glycosylated. A control protein, 11β-hydroxysteroid dehydrogenase type I, was efficiently deglycosylated by Endo H. To obtain further evidence for the lack of RalR1 glycosylation, we compared the electrophoretic mobility of ^{35}S-labeled RalR1 produced *in vitro* using a coupled transcription/translation system in the absence of microsomes (Fig. 3, *lane 4*) to that of the recombinant RalR1 expressed in Sf9 cell microsomes (Fig. 3, *lane 5*). Both samples were separated in the same gel and transferred to a nitrocellulose filter, which was then cut in half. The filter containing ^{35}S-labeled RalR1 was exposed to x-ray film, whereas the second filter was hybridized with anti-RalR1 mAbs to visualize the microsomal RalR1 by chemiluminescence. Alignment of the two images revealed that the microsomal RalR1 had electrophoretic mobility identical to that of RalR1 produced in the absence of microsomes (Fig. 3). To confirm this result, we compared the electrophoretic mobility of ^{35}S-labeled RalR1 preparations synthesized *in vitro* in the absence and presence of canine microsomal membranes. Canine microsomes efficiently glycosylated yeast α-mating factor, which was provided with the kit (data not shown), but RalR1 was not glycosylated. Because glycosylation occurs exclusively in the lumen of the ER, these results suggested that the segment of RalR1 containing the putative glycosylation motifs was not exposed to the ER lumen.

Analysis of RalR1 Substrate and Cofactor Specificity—Experiments were designed to compare the retinoid-metabolizing activity of Sf9 cells expressing RalR1 with the activity of Sf9 cells infected with wild-type virus. Homogenates of RalR1-Sf9 and virus-Sf9 cells were incubated with 1 μM all-*trans*-retinol or 1 μM all-*trans*-retinal in the presence of the oxidative (NAD$^+$/NADP$^+$) or reductive (NADH/NADPH) cofactors, respectively. The reaction products were extracted and analyzed by reverse-phase HPLC. In the oxidative direction, a maximum of only about 10% of substrate conversion was observed over a wide range of protein concentrations (up to 250 μg) (data not shown). However, when RalR1 was analyzed in the reductive direction, more than 90% of all-*trans*-retinal was converted to all-*trans*-retinol in the presence of NADPH (Fig. 4*A*). The same amount (micrograms) of homogenate obtained from control cells infected with wild-type virus produced at least 10-fold less all-*trans*-retinol (Fig. 4*B*). This result indicated that the observed retinal reductase activity was associated with RalR1. Percent conversion was generally lower in the presence of NADH for both RalR1- and wild-type virus infected cells (Fig. 4, *C* and *D*).

To determine whether retinal reductase activity colocalized with RalR1 protein in the microsomal fraction of the homogenate, we determined the activity of the subcellular fractions isolated from RalR1-expressing Sf9 cells. Similar to RalR1 protein distribution, over 90% of the retinal reductase was recovered with the microsomes (data not shown). No activity was detected in the microsomal fraction of Sf9 cells infected with wild-type virus, indicating that the low background activity observed with Sf9 cell homogenate in the presence of NADP$^+$ (Fig. 4) was due to the cytosolic enzymes. As determined by normal-phase HPLC analysis, the major product of all-*trans*-retinal reduction catalyzed by microsomal RalR1 was all-*trans*-retinol, although small amounts of 13-*cis* isomers of retinol and retinal were recovered as well (Fig. 5*A*). Isomerization of retinoids during extraction procedures was also observed by other investigators (10, 30). Therefore, the reaction products were quantified by summing the areas of both peaks.

The next question was whether RalR1 exhibited specificity for all-*trans*-retinal or whether it was also active toward *cis*-retinals. Kinetic analysis of the same preparation of microsomal RalR1 revealed that the enzyme recognized 9-*cis*-retinal and 13-*cis*-retinal as substrates with affinity similar to that for all-*trans*-retinal (K_m values of 0.19–0.62 μM) (Table I). How-

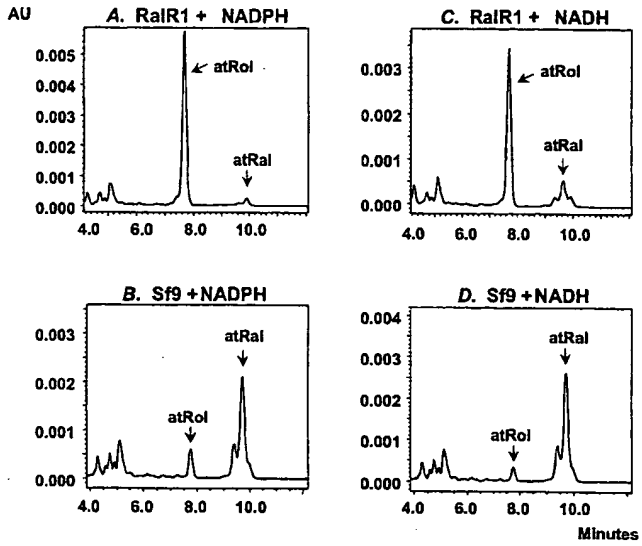

FIG. 4. **Reverse-phase HPLC analysis of the reductive activity of RalR1 toward all-*trans*-retinal.** Homogenates (250 μg per reaction) of Sf9 cells infected with RalR1 (*A* and *C*) or wild-type baculovirus (*B* and *D*) were incubated with 1 μM all-*trans*-retinal in the presence of 1 mM NADPH (*A* and *B*) or 1 mM NADH (*C* and *D*) for 30 min at 37 °C. The reactions were terminated by the addition of an equal volume of cold ethanol supplemented with 100 μg/ml butylated hydroxytoluene. Retinoids were extracted using solid-phase extraction on a Waters Sep-Pak C18 column as described before (27) and reconstituted into 200 μl of mobile phase acetonitrile:water:ammonium acetate (87.5:2.5:10.0, v/v). Ten-microliter aliquots were analyzed by reverse-phase HPLC using a 3.5-μm Waters Symmetry column (4.6 × 150 mm). The flow rate was 1 ml/min. Under these conditions, all-*trans*-retinol and all-*trans*-retinaldehyde eluted at 7.7 and 9.5 min, respectively.

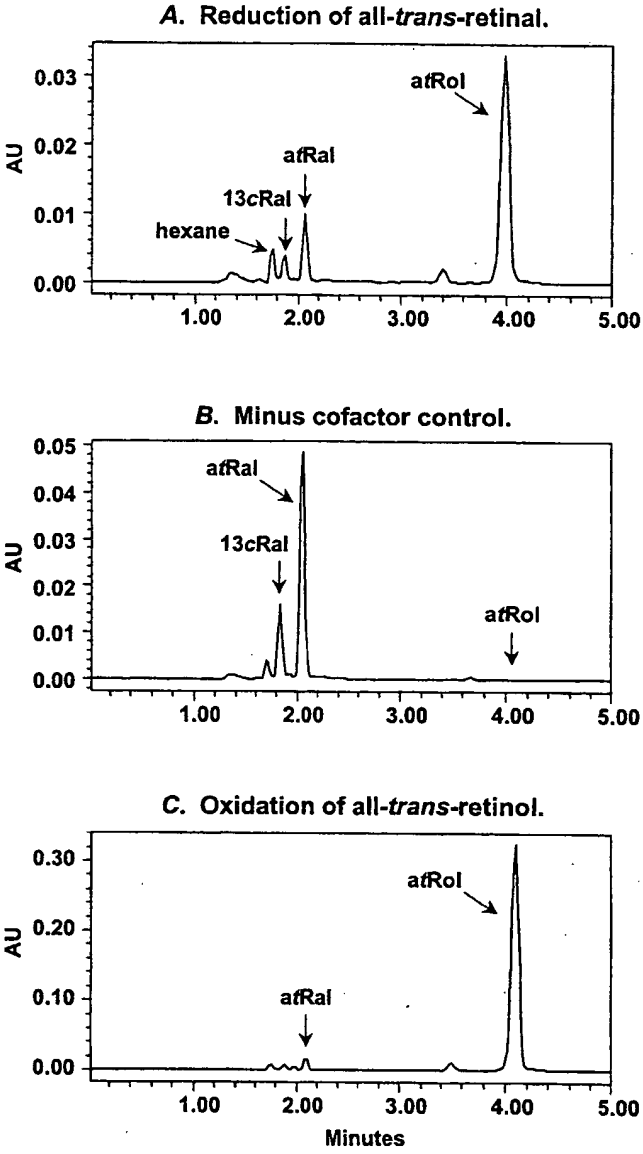

FIG. 5. **Normal-phase HPLC chromatogram of retinoids produced by RalR1 in the reductive and oxidative direction.** *A*, reduction of 1.25 μM all-*trans*-retinal to all-*trans*-retinol catalyzed by 10 μg of RalR1-containing Sf9 microsomes in the presence of 1 mM NADPH. All-*trans*-retinal partially isomerized into 13-*cis*-retinal during manipulations. *B*, the "minus cofactor control" for the reductive direction. *C*, oxidation of 10 μM all-*trans*-retinol to all-*trans*-retinal catalyzed by 7.5 μg of RalR1-containing Sf9 microsomes in the presence of 1 mM $NADP^+$.

ever, the reaction rate with *cis*-retinals was severalfold lower than with all-*trans*-retinal (Table I). Thus, RalR1 was most efficient as an all-*trans*-retinal reductase. In addition, the utilization ratio of RalR1 in the reductive direction was about 50-fold higher than in the oxidative direction with all-*trans*-retinol as substrate (Table I and Fig. 5*C*). The preference of RalR1 for the reductive direction was consistent with the apparent K_m values for cofactors. The enzyme exhibited a ~3000-fold lower K_m value for NADPH, the predominant reductive cofactor in the cells, than for NAD^+, the major oxidative cofactor (Table II).

Having established that RalR1 was most efficient as an all-*trans*-retinal reductase, we determined if RalR1 could function in the presence of cellular retinol binding protein, which was previously shown to completely sequester retinol and retinal from nonspecific enzymes (10, 28, 31). It was suggested that the microsomal retinal reductase activity previously described in the rat small intestine was important for retinoid metabolism, because, in contrast to the retinal reductase activity present in the cytosol, the microsomal activity reduced retinal in the presence of a 20% molar excess of CRBPII (10). The expression of CRBPII is restricted to the small intestine. Other tissues, including the prostate (32, 33), contain a different binding protein, CRBP type I, which binds all-*trans*-retinal and all-*trans*-retinol with even higher affinity than CRBPII (K_d values of 50 and <10 nM, respectively, compared with ~100 nM for CRBPII) (reviewed in Ref. 34). To determine whether RalR1 was capable of reducing all-*trans*-retinal in the presence of CRBPI, we titrated the reaction mixture with an increasing amount of the binding protein. As can be seen in Fig. 6, the addition of a 2.5-fold excess of CRBPI to the reaction mixture resulted in a decrease of ~6.5-fold in the rate of retinal reduction, from 8.5 nmol/min × mg at 1 μM all-*trans*-retinal down to 1.3 nmol/min × mg. However, further increases in the amount of added CRBPI had little effect on RalR1 activity. The reaction rate remained constant with up to a 10-fold molar excess of CRBPI relative to the retinal concentration (Fig. 6). This result indicated that RalR1 reduced retinal in the presence of a wide range of CRBPI concentrations.

Because several retinoid-metabolizing members of the SDR superfamily were shown to recognize 3α- and 17β-hydroxy and ketosteroids as substrates (24, 27, 35, 36), we tested whether RalR1 was also active toward steroids. Steroid compounds were used at a 1 μM concentration in the presence of either 1 mM NAD^+/$NADP^+$ or 1 mM NADH/NADPH. The reaction products were extracted and analyzed by TLC using a PhosphorImager. The oxidative retinol/sterol dehydrogenases characterized previously in our laboratory (24, 27) served as positive controls for steroid oxidoreductase activity. RalR1 did not possess any significant activity toward oxidation or reduction of the functional

TABLE I
Kinetic constants for retinoid substrates

Kinetic constants for the reduction of retinals were determined in the presence of saturating NADPH (0.5 mM). Kinetic constants for the oxidation of all-*trans*-retinol were determined at saturating NADP$^+$ (1 mM) (*Experimental Procedures*). Kinetic constants shown in this table were determined using the same preparation of microsomes containing RalR1 and were calculated using GraFit (Erithacus Software Ltd.) and expressed as the means ± S.D. Similar constants were obtained using three independent preparations of microsomal RalR1.

Substrate	Apparent K_m	Apparent V_{max}	V_{max}/K_m
	μM	*nmol/(min × mg microsomal protein)*	
All-*trans*-retinal	0.50 ± 0.05	18.0 ± 0.5	36
13-*cis*-retinal	0.62 ± 0.09	7.0 ± 0.3	11
9-*cis*-retinal	0.19 ± 0.04	1.6 ± 0.1	8.4
All-*trans*-retinol	1.3 ± 0.2	0.95 ± 0.04	0.7

TABLE II
Apparent K_m values for cofactors

The apparent K_m values for NADPH and NADH were determined with saturating all-*trans*-retinal (5 μM). The apparent K_m values for NADP$^+$ and NAD$^+$ were determined with saturating all-*trans*-retinol (15 μM) ("Experimental Procedures").

Cofactor	K_m
	μM
NADPH	0.23 ± 0.02
NADH	1300 ± 200
NADP	0.8 ± 0.2
NAD$^+$	680 ± 80

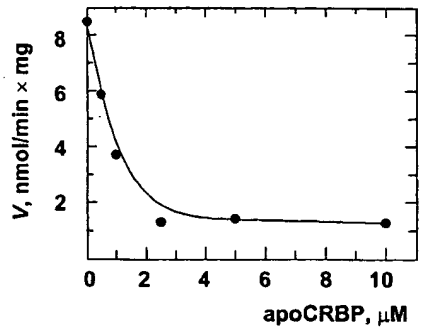

FIG. 6. **Analysis of RalR1 activity toward all-*trans*-retinal in the presence of CRBPI.** All-*trans*-retinal was used at a concentration of 1 μM. CRBPI concentration varied from 0.5 to 10 μM. The amount of microsomes in each 0.5-ml reaction was 2 μg. The result shown is representative of at least three independent experiments.

hydroxyl or ketone groups in positions 3, 17, or 20, relative to the background activity of Sf9 cells infected with wild-type virus (data not shown). Thus, RalR1 appeared to be specific for retinoids and was most efficient as an NADPH-dependent retinal reductase.

DISCUSSION

In the present study we have established that the protein encoded by the recently discovered human gene originally named *PSDR1* for prostate short-chain dehydrogenase/reductase encodes a novel microsomal enzyme with retinal reductase activity. Accordingly, we changed the designation of *PSDR1* gene and protein to *RalR1* for retinal reductase 1. RalR1 shares less than 30% overall sequence identity with other members of the SDR superfamily, including the recently characterized all-*trans*-retinal reductase retinal SDR1 (37) and the NADP$^+$-dependent photoreceptor-specific all-*trans*-retinol dehydrogenase photoreceptor retinol dehydrogenase (38). Analysis of the primary structure of RalR1 based on algorithms for secondary structure prediction (39, 40) suggests that RalR1 is a membrane protein anchored by a single hydrophobic N-terminal segment (amino acids 1–23) with the majority of the polypeptide chain localized on the cytosolic side of the membrane. This model is supported by the experimental data obtained in the present study. First of all, as established by cell fractionation and immunolocalization studies, RalR1 is associated with the ER membranes. Second, the subunit molecular weight of RalR1 does not change after incubation with microsomes, indicating that the ER targeting signal in RalR1 is not cleaved. Finally, RalR1 is not glycosylated at the putative *N*-linked glycosylation motifs at Asn^{174} and Asn^{298}. Because glycosylation occurs exclusively in the lumen of the ER, lack of glycosylation suggests that RalR1 faces the cytosolic side of the ER membrane.

The cytosolic orientation of RalR1 in the ER membrane suggests that in intact cells the enzyme will function as a reductase. RalR1 exhibits at least an 800-fold lower K_m values for NADP$^+$ and NADPH than for NAD$^+$ and NADH as cofactors. In the cytosol of liver and, presumably, other cells, NADP$^+$ exists mainly in the reduced form (41). Therefore, enzymes that prefer NADP$^+$ are likely to function in the reductive direction *in vivo*.

Characterization of RalR1 enzymatic properties revealed that the enzyme recognizes retinoids but not steroids as substrates and is particularly efficient as an all-*trans*-retinaldehyde reductase. Retinoids are highly hydrophobic and chemically labile compounds that are solubilized and protected from unwanted conversions by specific binding proteins inside the cells and in blood plasma (reviewed in Ref. 34). All-*trans*-retinal binds to cytosolic CRBPI, which is expressed in many different types of cells but the levels of CRBPI expression may vary (32). Most likely, the enzymes involved in retinoid metabolism have to function in the presence of some amount of CRBPI. Interestingly, not all enzymes that are active with free retinol can metabolize retinol in the presence of CRBPI. It was shown that CRBPI sequesters all-*trans*-retinol from acyl CoA: retinol acyltransferase (29, 31, 42, 43) and from human cytosolic alcohol dehydrogenase class IV (28), enzymes that are active with free retinol. On the other hand, retinal reductase activity in the rat intestine reduced all-*trans*-retinal in the presence of a 20% molar excess of CRBPII (10) and the cytosolic rat retinal dehydrogenase type 2 oxidized retinal in the presence of a 2-fold molar excess of CRBPI (3).

The ratio of CRBPI to retinaldehyde in the human prostate gland is not known. Kato *et al.* (32) reported that rat prostate contains an ~8-fold lower amount of CRBP than rat liver (5.2 *versus* 40.0 μg/g of wet weight). This translates into ~0.3 μM CRBP in rat prostate (molecular weight 14,600). The molar ratio of CRBP to retinal might vary, depending on the tissue supply of β-carotene and the rate of retinol oxidation to retinaldehyde. Therefore, we investigated the effect of CRBPI on RalR1 activity at a constant concentration of retinal over a wide range of CRBPI concentrations. Our results showed that RalR1 exhibits a relatively high rate (1.3 nmol/min × mg) of retinal reduction even at a 10-fold molar excess of CRBPI over 1 μM retinal concentration. Thus, RalR1 can produce retinol from retinaldehyde in the presence of varied physiological levels of CRBPI.

Retinoic acid plays an important role in the prostate as an activating ligand for retinoic acid receptor γ, which is required

for the normal differentiation of prostate epithelium (44). Accordingly, the prostate gland contains retinol dehydrogenase activity associated with the microsomes and retinal dehydrogenase activity in the cytosol that catalyze the formation of retinoic acid (45). Furthermore, a recent report demonstrated that prostate cells are capable of converting β-carotene to retinol, suggesting that these cells possess β-carotene dioxygenase and retinal reductase activities (22). While our manuscript was under revision, the presence of β-carotene dioxygenase (β-carotene 15,15′-monooxygenase) mRNA in human prostate was directly demonstrated in a study by Lindqvist and Andersson (46), providing further support for colocalization of β-carotene dioxygenase and retinal reductase.

Under normal circumstances, the intracellular levels of retinoic acid in tissues are tightly controlled. The molecular mechanisms responsible for this regulation are not yet fully understood but appear to function at several levels of retinoic acid metabolism: biosynthesis, degradation, and storage. Aberrations in retinoid signaling are early events in carcinogenesis, and vitamin A deficiency has been associated with a higher incidence of cancer (reviewed in Ref. 47). It has been demonstrated that the levels of retinoic acid are five to eight times lower in human prostate cancer than in normal prostate cells (45). Supplementation of the diet with β-carotene appears to decrease the risk of developing prostate cancer (48), and it was shown that β-carotene inhibits the growth of prostate cancer cells *in vitro* (22).

From a metabolic point of view, retinal produced from β-carotene in the prostate or any other peripheral tissue may be either oxidized to bioactive retinoic acid by cytosolic aldehyde dehydrogenases or it may be reduced to retinol, which can then be esterified for storage (8). Hence, retinal is positioned at the crossroads of two opposite metabolic processes: activation and inactivation of retinoids. The fate of the cellular retinal would depend on the activities and expression levels of local aldehyde dehydrogenases and retinal reductases that compete for the same all-*trans*-retinal substrate. Therefore, changes in the expression level of RalR1 could perturb retinoid homeostasis and alter the intracellular retinoic acid concentrations, leading to abnormal differentiation of prostate epithelium.

Besides prostate, RalR1 appears to be expressed at lower levels in a number of different human tissues, including the small intestine (23), where it could play a role in retinoid metabolism. Identification and characterization of retinal reductases in human tissues will provide a better understanding of the control mechanisms responsible for the regulation of intracellular retinoic acid concentrations.

Acknowledgments—We thank Larry True for assistance with immunohistochemistry, and we thank Robert Vessella and the Department of Urology at the University of Washington for providing prostate tissues. We are grateful to Dr. Kirill Popov for a critical reading of the manuscript.

REFERENCES

1. Mangelsdorf, D., Umesono, K., and Evans, R. M. (1994) in *The Retinoids: Biology, Chemistry and Medicine* (Sporn, M. B., Roberts, A. B., and Goodman, D. S., eds) pp. 319–350, Raven Press, New York
2. Zhao, D., McCaffery, P., Ivins, K. J., Neve, R. L., Hogan, P., Chin, W. W., and Drager, U. C. (1996) *Eur. J. Biochem.* **240,** 15–22
3. Wang, X., Penzes, P., and Napoli, J. L. (1996) *J. Biol. Chem.* **271,** 16288–16293
4. Ambroziak, W., Izaguirre, G., and Pietruszko, R. (1999) *J. Biol. Chem.* **274,** 33366–33373
5. Grün, F., Hirose, Y., Kawauchi, S., Ogura, T., and Umesono, K. (2000) *J. Biol. Chem.* **275,** 41210–41218
6. Napoli, J. L. (1999) *Biochim. Biophys. Acta* **1440,** 139–162
7. Duester, G. (2000) *Eur. J. Biochem.* **267,** 4315–4324
8. Blaner, W. S., and Olson, J. A. (1994) in *The Retinoids: Biology, Chemistry and Medicine* (Sporn, M. B., Roberts, A. B., and Goodman, D. S., eds) pp. 229–250, Raven Press, New York
9. Barua, A. B., and Olson, J. A. (2000) *J. Nutr.* **130,** 1996–2001
10. Kakkad, B. P., and Ong, D. E. (1988) *J. Biol. Chem.* **263,** 12916–12919
11. Li, E., Demmer, L. A., Sweetser, D. A., Ong, D. E., and Gordon, J. I. (1986) *Proc. Natl. Acad. Sci. U. S. A.* **83,** 5779–5783
12. Vogel, S., Gamble, M. V., and Blaner, W. S. (1999) in *Retinoids: The Biochemical and Molecular Basis of Vitamin A and Retinoid Action*, Vol. 139 (Nau, H., and Blaner, W. S., eds.), pp. 31–96, Springer-Verlag, Berlin
13. During, A., Albaugh, G., and Smith, J. C. (1998) *Biochem. Biophys. Res. Commun.* **249,** 467–474
14. Scita, G., Aponte, G. W., and Wolf, G. (1992) *J. Nutr. Biochem.* **3,** 118–123
15. Wei, R. R., Wamer, W. G., Lambert, L. A., and Kornhauser, A. (1998) *Nutr. Cancer* **30,** 53–58
16. von Lintig, J., and Vogt, K. (2000) *J. Biol. Chem.* **275,** 11915–11920
17. Wyss, A., Wirtz, G., Woggon, W., Brugger, R., Wyss, M., Friedlein, A., Bachmann, H., and Hunziker, W. (2000) *Biochem. Biophys. Res. Commun.* **271,** 334–336
18. Redmond, T. M., Gentleman, S., Duncan, T., Yu, S., Wiggert, B., Gantt, E., and Cunningham, F. X., Jr. (2001) *J. Biol. Chem.* **276,** 6560–6565
19. Paik, J., During, A., Harrison, E. H., Mendelsohn, C. L., Lai, K., and Blaner, W. S. (2001) *J. Biol. Chem.* **276,** 32160–32168
20. Yan, W., Jang, G. F., Haeseleer, F., Esumi, N., Chang, J., Kerrigan, M., Campochiaro, M., Campochiaro, P., Palczewski, K., and Zack, D. J. (2001) *Genomics* **72,** 193–202
21. Wyss, A., Wirtz, G. M., Woggon, W. D., Brugger, R., Wyss, M., Friedlein, A., Riss, G., Bachmann, H., and Hunziker, W. (2001) *Biochem. J.* **354,** 521–529
22. Williams, A. W., Boileau, T. W.-M., Zhou, J. R., Clinton, S. K., and Erdman, J. W. (2000) *J. Nutr.* **130,** 728–732
23. Lin, B., White, J. T., Ferguson, C., Wang, S., Vessella, R., Bumgarner, R., True, L. D., Hood, L., and Nelson, P. S. (2001) *Cancer Res.* **61,** 1611–1618
24. Gough, W. H., VanOoteghem, S., Sint, T., and Kedishvili, N. Y. (1998) *J. Biol. Chem.* **273,** 19778–19785
25. Lowry, O. H., Rosebrough, N. H., Farr, A. L., and Randall, R. J. (1951) *J. Biol. Chem.* **193,** 265–275
26. Chetyrkin, S. V., Belyaeva, O. V., Gough, W. H., and Kedishvili, N. Y. (2001) *J. Biol. Chem.* **276,** 22278–22286
27. Chetyrkin, S. V., Hu, J., Gough, W. H., Dumaual, N., and Kedishvili, N. Y. (2001) *Arch. Biochem. Biophys.* **386,** 1–10
28. Kedishvili, N. Y., Gough, W. H., Davis, W. I., Parsons, S., Li, T. K., and Bosron, W. F. (1998) *Biochem. Biophys. Res. Commun.* **249,** 191–196
29. Ong, D. E., Kakkad, B., and MacDonald, P. N. (1987) *J. Biol. Chem.* **262,** 2729–2736
30. Gamble, M. V., Shang, E., Zott, R. P., Mertz, J. R., Wolgemuth, D. J., and Blaner, W. S. (1999) *J. Lipid Res.* **40,** 2279–2292
31. Randolph, R. K., Winkler, K. E., and Ross, A. C. (1991) *Arch. Biochem. Biophys.* **288,** 500–508
32. Kato, M., Blaner, W. S., Mertz, J. R., Das, K., Kato, K., and Goodman, D. S. (1985) *J. Biol. Chem.* **260,** 4832–4838
33. Pasquali, D., Rossi, V., Prezioso, D., Gentile, V., Colantuoni, V., Lotti, T., Bellastella, A., and Sinisi, A. A. (1999) *J. Clin. Endocrinol. Metab.* **84,** 1463–1469
34. Noy, N. (2000) *Biochem. J.* **348,** 481–495
35. Biswas, M. G., and Russell, D. W. (1997) *J. Biol. Chem.* **272,** 15959–15966
36. Wang, J., Chai, X., Eriksson, U., and Napoli, J. L. (1999) *Biochem. J.* **338,** 23–27
37. Haeseleer, F., Huang, J., Lebioda, L., Saari, J. C., and Palczewski, K. (1998) *J. Biol. Chem.* **273,** 21790–21799
38. Rattner, A., Smallwood, P. M., and Nathans, J. (2000) *J. Biol. Chem.* **275,** 11034–11043
39. von Heijne, G. (1992) *J. Mol. Biol.* **225,** 487–494
40. Claros, M. G., and von Heijne, G. (1994) *Comput. Appl. Sci.* **10,** 685–686
41. Veech, R. L., Eggleston, L. V., and Krebs, H. A. (1969) *Biochem. J.* **115,** 609–619
42. Ong, D. E., MacDonald, P. N., and Gubitosi, A. M. (1988) *J. Biol. Chem.* **263,** 5789–5796
43. Yost, R. W., Harrison, E. H., and Ross, A. C. (1988) *J. Biol. Chem.* **263,** 18693–18701
44. Lohnes, D., Kastner, P., Dierich, A., Mark, M., LeMeur, M., and Chambon, P. (1993) *Cell* **73,** 643–658
45. Pasquali, D., Thaller, C., and Eichele, G. (1996) *J. Clin. Endocrinol. Metab.* **81,** 2186–2191
46. Lindqvist, A., and Andersson, S. (2002) *J. Biol. Chem.* **277,** 23942–23948
47. Sun, S. Y., and Lotan, R. (2002) *Crit. Rev. Oncol. Hematol.* **41,** 41–55
48. Cook, N. R., Stampfer, M. J., Ma, J., Manson, J. E., Sacks, F. M., Buring, J. E., and Hennekens, C. H. (1999) *Cancer* **86,** 1783–1792